A defective ABC transporter of the MRP family, responsible for the bean *lpa1* mutation, affects the regulation of the phytic acid pathway, reduces seed *myo*-inositol and alters ABA sensitivity

Dario Panzeri[1], Elena Cassani[2], Enrico Doria[3], Giovanni Tagliabue[1], Luca Forti[4], Bruno Campion[5], Roberto Bollini[1], Charles A. Brearley[6], Roberto Pilu[2], Erik Nielsen[3] and Francesca Sparvoli[1]

[1]Istituto di Biologia e Biotecnologia Agraria, CNR, Milano, Italy; [2]Dipartimento di Produzione Vegetale, Università degli Studi di Milano, Italy; [3]Dipartimento di Genetica e Microbiologia, Università di Pavia, Pavia, Italy; [4]Dipartimento di Chimica, Università di Modena, Modena, Italy; [5]Unità di ricerca per l'Orticoltura CRA, Montanaso Lombardo, Lodi, Italy; [6]School of Biological Sciences, University of East Anglia, Norwich NR4 7TJ, UK

Summary

• We previously identified the *lpa1* (low phytic acid) 280-10 line that carries a mutation conferring a 90% reduction in phytic acid (InsP$_6$) content. In contrast to other *lpa* mutants, *lpa1*(280-10) does not display negative pleiotropic effects. In the present paper, we have identified the mutated gene and analysed its impact on the phytic acid pathway.

• Here, we mapped the *lpa1*(280-10) mutation by bulk analysis on a segregating F$_2$ population, an then, by comparison with the soybean genome, we identified and sequenced a candidate gene. The InsP$_6$ pathway was analysed by gene expression and quantification of metabolites.

• The mutated *Pvmrp1*(280-10) cosegregates with the *lpa1*(280-10) mutation, and the expression level of several genes of the InsP$_6$ pathway are reduced in the *lpa1*(280-10) mutant as well as the inositol and raffinosaccharide content. *PvMrp2*, a very similar paralogue of *PvMrp1* was also mapped and sequenced.

• The *lpa1* mutation in beans is likely the result of a defective *Mrp1* gene (ortho-logous to the *lpa* genes *AtMRP5* and *ZmMRP4*), while its *Mrp2* paralog is not able to complement the mutant phenotype in the seed. This mutation appears to down-regulate the InsP$_6$ pathway at the transcriptional level, as well as altering inositol-related metabolism and affecting ABA sensitivity.

Abbreviations: ABC, ATP-binding cassette; MRP, multidrug resistance-associated protein; InsP$_6$, *myo*-inositol-1,2,3,4,5,6-hexa*kis*phosphate; IMP, *myo*-inositol-phosphate monophosphatase; MIPS, *myo*-inositol-3-phosphate synthase; MIK, *myo*-inositol kinase; IPK2, inositol 1,4,5-tris-phosphate kinase; ITPK, inositol 1,3,4-triphosphate 5/6-kinase; IPK1, inositol 1,3,4,5,6 penta*kis*phosphate 2-kinase.

Introduction

Phytic acid (*myo*-inositol-1,2,3,4,5,6-hexa*kis*phosphate; InsP$_6$) is the main storage form for phosphate in plant seeds which accumulates in the protein storage vacuole in inclusions called globoids. Phytic acid is poorly digested by monogastric animals and humans and decreases the nutritional value of the seeds by trapping phosphate and chelating nutritionally important minerals, such as iron, zinc, magnesium, and calcium. Therefore, the isolation of *low phytic acid* (*lpa*) mutants is considered a highly desirable objective in the genetic improvement of the nutritional quality of grain crops (Raboy, 2006), also considering the correlation between InsP$_6$ reduction in *lpa* seeds and increased phosphate and mineral cation bioavailability demonstrated in nutritional trials (Mendoza *et al.*, 1998;

Hambidge *et al.*, 2004, 2005). These mutants have been isolated in important crops such as maize, barley, rice, wheat, soybean (reviewed by Cichy & Raboy, 2009) and, by our research group, common bean (Campion *et al.*, 2009), a legume entirely used for human consumption which represents a very important source of nutrients for resource-poor people worldwide.

The *lpa* mutations characterized so far affect the partitioning of P into $InsP_6$, inorganic phosphorus (P_i) and inositol phosphates (InsPs) with five or fewer P esters (Raboy, 2002), and fall into three classes: mutations affecting the early part of the phytic acid biosynthetic pathway, with decreased $InsP_6$ and a molar equivalent increase in inorganic P_i; mutations in the late part of the pathway, with decreased $InsP_6$ matched by increases in both P_i and lower InsPs; and mutations affecting the transport of phytic acid to the vacuole. Mutants in the early pathway carry defective structural genes needed for *myo*-inositol synthesis and subsequent phosphorylation. These include *myo*-inositol-3-phosphate synthase, *myo*-inositol kinase and 2-phosphoglycerate kinase (Hitz *et al.*, 2002; Shi *et al.*, 2005; Kim *et al.*, 2008). Conversely, mutants of the late part of the pathway are altered in one of the genes coding for inositol kinases involved in the sequential phosphorylation steps of $InsP_3$, $InsP_4$ and/or $InsP_5$ intermediates (reviewed by Cichy & Raboy, 2009). Mutants in phytic acid vacuolar storage have a nonfunctional multidrug resistance-associated protein (MRP) type ATP-binding cassette (ABC) transporter which is a high-affinity $InsP_6$ transporter (ABCC5) (Shi *et al.*, 2007; Nagy *et al.*, 2009; Xu *et al.*, 2009).

From an agronomical point of view, *lpa* mutants are often associated with negative effects on seed and plant performance, such as compromised germination and emergence, lower stress tolerance and poor seed filling (Meis *et al.*, 2003; Pilu *et al.*, 2005; Bregitzer & Raboy, 2006; Guttieri *et al.*, 2006). Although there are some exceptions, like the *Arabidopsis* mutant *Atmrp5* (bearing a mutation in the $InsP_6$ transporter), which is drought-tolerant (Klein *et al.*, 2003), or the barley *lpa1-1*, which showed a good agronomic performance in both irrigated and nonirrigated environments (Bregitzer & Raboy, 2006), projects aimed at obtaining *lpa* crops should take into account aspects regarding agronomic potential.

Recent papers suggest a correlation between *myo*-inositol content and response to ABA during seed germination. In fact, *Arabidopsis mips1* and *vtc4* mutants (mutated in *myo*-inositol-3-phosphate synthase and inositol-phosphate monophosphatase, respectively), have impaired germination in response to ABA, a phenotype which correlates with reduced *myo*-inositol seed content (Torabinejad *et al.*, 2009; Donahue *et al.*, 2010). Conversely, seeds of *Arabidopsis* lines overexpressing the *AtPAP15* gene, coding for a purple acid phosphatase with a phytase activity, have been shown to be ABA-insensitive (Zhang *et al.*, 2008).

These plants show a 20–30% decrease in foliar phytate and a twofold increase in foliar ascorbic acid, possibly because of an increase in *myo*-inositol that is also a substrate for ascorbic acid biosynthesis (Lorence *et al.*, 2004). Interestingly, an altered ABA phenotype during germination was also reported for the *Arabidopsis mrp5* mutant which was shown to be ABA-insensitive (Klein *et al.*, 2003). Most likely, all the above pleiotropic effects could be explained by the fact that metabolites of the phytic acid pathway, such as *myo*-inositol, $Ins(1,4,5)P_3$ and $InsP_6$ itself, have been shown to play a key regulatory role in signal transduction and in the control of plant response to environmental stresses (Munnik & Vermeer, 2010).

We previously (Campion *et al.*, 2009) presented data on the isolation and initial characterization of the common bean *lpa*-280-10 mutant, which, in accordance with the *Phaseolus* nomenclature guidelines, is hereafter referred to as *lpa1*(280-10). This mutant shows several nutritionally important characteristics, such as a 90% reduction in $InsP_6$, a 25% reduction in raffinosaccharide content and sevenfold increase of free iron cations in the seeds. We also provided evidence that, unlike other 'strong' *lpa* mutants (having up to 90% of phytic acid reduction), *lpa1*(280-10) shows no negative pleiotropic effects on traits of agronomic relevance. In this study we have mapped the *lpa1*(280-10) mutation to the bean chromosome 1 and demonstrated that it is associated with a defective MRP type ABC transporter gene (*Pvmrp1*), orthologous to *Arabidopsis AtMRP5/AtABCC5* and maize *ZmMRP4* (*lpa1*). Investigations at biochemical and molecular levels aimed at assessing the effects of the *lpa1*(280-10) mutation on the amounts of some metabolites and on the expression of genes involved in the phytic acid pathway showed that the *Pvmrp1* mutation determines a general repression of the pathway, indicating that transient accumulation of $InsP_6$, or products derived from its degradation, may reduce its biosynthesis through a negative feedback mechanism. Moreover, we detected increased ABA sensitivity during germination of the mutant that apparently correlates with the lower *myo*-inositol content observed in the in *lpa1*(280-10) seeds, a finding supported by data on *Arabidopsis* mutants with reduced *myo*-inositol content (Zhang *et al.*, 2008; Torabinejad *et al.*, 2009; Donahue *et al.*, 2010).

Materials and Methods

Plant material

Plants (*Phaseolus vulgaris* L.) of *lpa1*(280-10) mutant line or parental line 905 (Campion *et al.*, 2009) were grown in phytotron under a 16 : 8 h light : dark photoperiod, with temperatures set at 25 : 18°C day : night and a relative humidity of *c*. 65%. Seeds and pods were collected on different days after flowering (DAF). At 4–6 DAF only pods

could be collected, while after 12 DAF cotyledons could be dissected from the tegument and embryo. Leaves and roots were collected from adult plants. All samples were immediately frozen in liquid nitrogen and stored at −80°C until use.

Labelling of leaf tissue and developing cotyledons

Leaf discs were cut from wild-type (wt) and *lpa1*(280-10) leaves. Six discs were incubated on 3 ml of 10 mM KCl, 0.1 mM CaCl$_2$, 50 mM MES2-(N-morpholino)ethane-sulfonic acid, pH 5.6, containing 1.85 MBq of *myo*-[2-^{3}H]inositol, specific activity 752 GBq mmol^{-1} (PerkinElmer, Boston, MA, USA). For analysis, two discs were washed in water, blotted dry and extracted. Developing seeds were labelled for periods up to 72 h with 1.85 Mq (50 μl) of *myo*-[2-^{3}H]inositol applied directly to the inner faces of half cotyledons. For analysis, three cotyledons were washed briefly in water, blotted dry and extracted.

High-performance liquid chromatography (HPLC) analyses of inositol phosphates

Mature seed flours were extracted with 40 vol of 0.4 M HCl, overnight at 4°C under shaking. Samples were centrifuged 10 min at 12 000 *g* and the supernatant was filtered on a Millipore 0.45 μm filter. Quantification of InsPs was carried out by metal-dye detection (MDD)-HPLC analysis as described in Bohn *et al.* (2007).

Extracts from developing seeds and leaves were analysed on a 25 cm × 4 mm Dionex (Sunnyvale, CA, USA) AS11 column fitted with AG11 guard cartridge eluted at a flow rate of 1 ml min^{-1}. Samples (100 μl) were loaded and eluted with a NaOH gradient generated by mixing solvents from buffer reservoirs (A, water; B, 150 mM NaOH), as follows (time (min), %B): 0, 3.3; 5, 3.3; 22.5, 35; 22.6,100; 27, 100; 27.1, 3.3; 0; 40, 3.3. Peaks of ions were detected by suppressed ion conductivity on the ED40 detector of a Dionex DX500 chromatography system fitted with an anion micromembrane suppressor operated at 100 mA suppressor current. In some experiments, eluent from the suppressor was analysed for radioactivity after admixture of scintillation fluid at a flow rate of 1 ml min^{-1}. Radiolabelled InsPs extracts were analysed according to Nagy *et al.* (2009). All data were exported and redrawn in Delta Graph 4.0.

GC-MS analyses of *myo*-inositol

Seed flours were extracted with 10 vol of 50% aqueous ethanol. After 1 h at room temperature the extract was decanted through a 0.45 μm nylon syringe filter attached to a 1 ml syringe barrel. Residue was re-extracted with 1 ml of fresh 50% aqueous ethanol and the second extract was filtered as before. The combined filtrates were evaporated to dryness. The *myo*-inositol derivative was produced by redissolving

the residues in 50 μl of pyridine and 50 μl of trimethylsilyl-imidazole : trimethylchlorosilane (100 : 1). After 15 min at 60°C, 1 ml of 2,2,4-trimethylpentane and 0.5 ml of distilled water were added, the sample was vortexed and centrifuged for 5 min, and the upper organic layer was transferred into 2 ml glass vial.

Myo-inositol was quantified as a hexa-trimethylsilyl ether derivative by GC-MS (G1800C Series II instrument; Hewlett Packard, Palo Alto, CA, USA). Samples were injected split mode (split ratio 10) with the injector temperature at 250°C and the oven at 70°C. After 2 min, the oven temperature was ramped at 25°C min^{-1} to 170°C, then continued at 5°C min^{-1} to 215°C and finally increased at 25°C min^{-1} to 250°C and returned to the initial temperature. Electron impact mass spectra from *m/z* 50–560 were acquired at −70 eV after a 5 min solvent delay. *Myo*-inositol hexa-trimethylsilyl ether was identified by comparing the mass fragmentation pattern with the database library NIST05 (MS Library Software Varian, Palo Alto, CA, USA). Authentic *myo*-inositol standards in aqueous solutions were dried, derivatized and analysed at the same time. Concentrations of *myo*-inositol were calculated from the standard curve, obtained using the external standard method.

lpa1(280-10) mapping

To map the recessive *lpa1*(280-10) mutation, we produced an F$_2$-segregating population by selfing hybrid plants Jalo EEP558 × *lpa1*(280-10). Flours of F$_2$ seeds were assayed for the high inorganic phosphate (HIP) phenotype as in Campion *et al.* (2009). Samples of the same flours were also used for DNA extraction using the GenElute™ Plant Genomic DNA Miniprep Kit (Sigma, St. Louis, MO, USA).

We used bulk segregant analysis to identify the approximate chromosomal region where the *lpa1*(280-10) mutation is located. Two DNA bulks were prepared: bulk A, obtained from a pool of 15 wt F$_2$ seeds, and bulk B, obtained from a pool of 15 HIP F$_2$ seeds. Both samples were amplified using the 19 simple sequence repeat (SSR) markers that were polymorphic on the parental lines (Supporting Information, Table S1) among 47 markers distributed over the entire genome (Grisi *et al.*, 2007). A map was then generated by testing the entire F$_2$ population using the linked SSR markers.

Polymerase chain reaction were performed in a final volume of 10 μl, containing 10 ng DNA, 0.1 μM of each primer, 200 mM of each dNTP, 2.5 mM MgCl$_2$ and one unit of Taq DNA polymerase (Promega, Madison, WI, USA). The reactions were carried out as follows: 94°C for 1 min, 35 cycles at 94°C for 1 min, 56°C for 1 min, 72°C for 1 min, and a final step at 72°C for 7 min. The amplified fragments were resolved on 4% agarose gels. Recombinant values were converted to map distances using MAPMAKER 3 (Lander *et al.*, 1987).

PvMrp1 and PvMrp2 gene sequence analysis and marker development

PaMRP4-F and PaMRP4-R primers (Tables S2) were designed on the conserved regions among the soybean *MRP* sequence (CS229850) described by Shi *et al.* (2007), the maize *ZmMRP4* sequence and a *Phaseolus acutifolius* expressed sequence tag (EST) sequence (CX129901), which shares *c.* 80% of sequence identity with the soybean *MRP*. PCR reactions were carried out as described earlier (melting temperature T_m = 50°C). The amplified fragment was sequenced and then used to screen a bean Bacterial Artificial Chromosome (BAC) library (Galasso *et al.*, 2009) for *PvMrp*-containing clones.

The partial bean *Mrp* sequence was aligned to *Gm03g32500*, *Gm19g35230* and *Gm13g18960 MRP* genes and the multiple alignment was used for further primer design (Table S3). To discriminate between the two homologue *PvMrp* genes, primers were always tested for amplification on *PvMrp1*- and *PvMrp2*-specific BAC clones, and then used for cDNA and genomic DNA amplification from both wt and *lpa1*(280-10) plants. Raw sequences of the amplified fragments (Table S2) were assembled and managed using the Vector NTI Advance 9.0 software (Invitrogen, Paisley, UK). Sequences have been deposited in GenBank database under ID FR694187 (*PvMrp1*), FR694188 (*PvMrp2*).

Cosegregation analysis

Cosegregation analysis between *lpa* phenotype and *PvMrp1* sequence was performed using the primers pol_19.03f and pol_19.04r (Table S3) to obtain allele-specific amplified products. PCR reactions were carried out as above (T_m = 52°C).

PvMrp2 sequence mapping

In order to map the *PvMrp2* sequence, we amplified a portion of this gene using the primers pol1F and pol1R (Table S3) to obtain allele-specific products of 122 bp for the *PvMrp2*(Jalo EEP558) allele and 131 bp for the *PvMrp2*(280-10) allele. PCR reactions were carried out as described earlier (T_m = 52°C).

Samples from flour bulk A and B (see earlier in the *lpa1*(280-10) mapping section) yielded 122 bp and 131 bp amplified products, respectively. Both samples were amplified using the 19 polymorphic SSR markers and the map was created testing the entire F_2 population with the linked SSR markers as described earlier for the *lpa1*(280-10) mapping.

Northern blot analysis and semiquantitative RT-PCR

Total RNA was isolated from leaves, roots, immature pods or cotyledons as described by van Tunen *et al.* (1988). Ten micrograms from each sample were resolved on 1.2% agarose/formaldehyde/3-[N-Morpholino]-propanesulfonic acid (MOPS) gel and transferred to a nylon membrane (Hybond™ N⁺; GE Healthcare, Uppsala, Sweden). The isolated cDNA sequences of genes for phytic acid synthesis (Fileppi *et al.*, 2010) and the one coding for phaseolin storage protein (Slightom *et al.*, 1985) were labelled with α-[^{32}P]-dCTP using a random primer DNA labelling kit (Fermentas, Burlington, Ontario, Canada) and used for membrane hybridizations (Sparvoli *et al.*, 1994). The membrane was washed at 0.2 × saline-sodium citrate buffer (SSC), 0.5% (w/v) sodium dodecyl sulfate (SDS) at 65°C.

Semiquantitative reverse transcriptioin (RT)-PCR and RT-PCR analysis were performed according to Fileppi *et al.* (2010). *PvMrp1* and *PvMrp2* were amplified using primers 42f, 41r (T_m = 54°C) and PaMRP4-F, pol1R (T_m = 50°C) (Table S3); the PCR amplification programme for both transcripts was: 37 cycles at 94°C for 30 s, T_m for 30 s, 72°C for 50 s, and a final step at 72°C for 7 min.

Seed germination assay

One hundred seeds of wt or *lpa1*(280-10) lines were imbibed in 70 ml water or solutions of different ABA concentrations (2.5, 5, 25, 50, 100, 250 μM) in 20-cm-diameter Petri dishes at 25°C in the dark. Counts of germinating seeds were made once a day, starting on the first day and until the maximum of germination was achieved.

Results

Metabolic characterization of the mutant line lpa1(280-10)

To gain information on the *lpa* mutation, we first performed a suppressed anion conductivity HPLC analysis (Fig. 1a,b). On the AS11 column used here, D/L-Ins(1,2,4,5,6)P_5 and Ins(1,3,4,5,6)P_5 elute after InsP_6 (Casaravilla *et al.*, 2006), as do some InsP_4s (C. Brearley, unpublished). A peak co-eluting precisely with InsP_6 was detected in developing seeds of wt, but was absent from *lpa1*(280-10). In parallel HPLC runs to that shown in the figure, we have shown that the principal component in a commercial sample of Ins1P eluted at 11.2 min, while Ins(1,4)P_2 gave a peak at 14.7 min. While there are peaks in the chromatograms (Fig. 1a,b) with similar retention times, we are unable to conclude that they are InsPs (stereoisomerism unknown) set against the likely presence of many anions in the extracts. Further analysis of flours from mature seeds was performed by MDD-HPLC (Fig. 1c,d). Contrary to what was found in the case of *lpa* mutants affected in *myo*-inositol phosphate kinases acting in the late pathway, no peaks corresponding to lower InsPs were visible in the chromatograms of wt or mutant flours
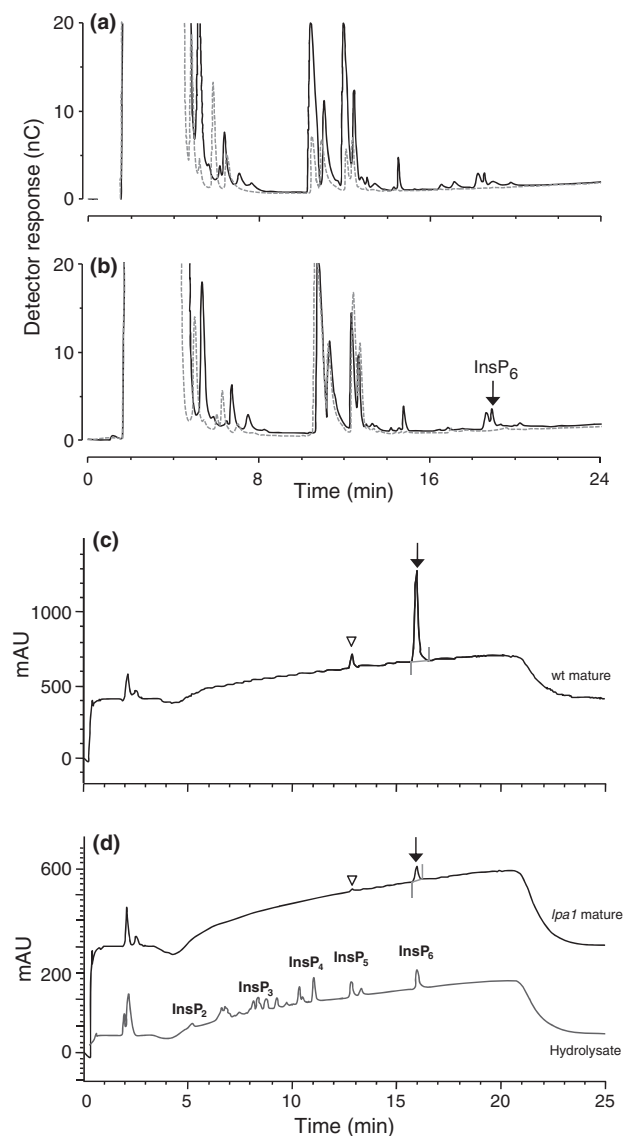
Fig. 1 Conductivity high-performance liquid chromatography (HPLC) profiles (a, b) and metal-dye detection (MDD)-HPLC profiles (c, d) of extracts from wild-type (wt) and *lpa1*(280-10) seeds at different developmental stages. Conductivity profiles of extracts from developing seeds at 18 d after flowering (DAF) (a) and 21 DAF (b) (*lpa1*(280-10), dotted grey lines; wt, black lines). MDD-HPLC profiles from mature seeds, wt (c), *lpa1*(280-10) (d) (mAU, arbitrary units). A number of standards obtained from an hydrolysate of phytic acid (InsP$_6$) are shown (d). Arrows indicate InsP$_6$ peaks; arrowheads indicate InsP$_5$ peaks. At maturity, *lpa1*(280-10) seeds contain very low concentrations of InsP$_6$ while InsP$_5$ is almost undetectable.

(Fig. 1c,d). The absence of lower InsPs is typical of *lpa* mutants of early steps of InsP$_6$ biosynthesis and of mutations of the phytic acid ATP-binding cassette transporter (Raboy *et al.*, 2000; Hatzack *et al.*, 2001; Dorsch *et al.*, 2003; Raboy, 2006; Nagy *et al.*, 2009).

A consequence of the *myo*-inositol-3-phosphate synthase (MIPS) gene mutation in the soybean L33 mutant is a significant reduction in the total raffinosaccharide synthesis (Hitz

et al., 2002). As *myo*-inositol-3-phosphate, the product of the MIPS, is the only known precursor for the *de novo* synthesis of *myo*-inositol, we reasoned that a strong reduction in the amount of this latter important metabolite might be detected in *lpa1*(280-10) seeds if the mutation had affected MIPS activity. Data obtained by GC-MS analysis showed that the amount of *myo*-inositol detectable in *lpa1*(280-10) grains is reduced (30% decrease) compared with wt grains (Fig. 2).

lpa1(280-10) mutation mapping

To map *lpa1*(280-10) mutation, we used a DNA bulks strategy to reduce the number of PCR reactions required. We selected 19 polymorphic SSR markers out of 47 (28 SSRs proved monomorphic) to establish linkage. The molecular markers *PV31*, *PV218*, *PV133* and *BM53* showed a clear bias towards a *lpa1*(280-10)-specific band in the mutant pool as compared with the wt pool, indicating that the mutation maps on chromosome 1. Using these markers, an F$_2$ mapping population of 198 individuals was screened for recombinants for each SSR marker and the values obtained were converted to map distances using MAPMAKER 3 (Lander *et al.*, 1987). Mapping data established the position of the mutation at a distance of *c.* 2.8 cM from *PV31* and *PV218*, 5.4 cM from *PV133* and 4.8 cM from *BM53* (Fig. 3a).

To identify the gene responsible of the *lpa1*(280-10) mutation, we took advantage of the high synteny between soybean and common bean genomes (Choi *et al.*, 2004). We used an *in silico* approach to identify which region of soybean genome corresponded to the one identified by the SSR markers closer to the *lpa1*(280-10) mutation. The results of the comparative mapping analysis allowed the identification of two syntenic regions of *c.* 3.3 Mbp, delimited by the *PV31* and *PV133* homologues on soybean chromosomes 3 and 19 (Table 1). These two regions contain two putative MRP proteins that we refer to as GmMRP03 and GmMRP19 (coded by *Gm03g32500* and *Gm19g35230*), which have recently been reported to be mutated in the soybean *lpa* CX1834 (Gillman *et al.*, 2009; Saghai Maroof *et al.*, 2009). A third putative MRP protein, GmMRP13 (*Gm13g18960*), is found on soybean chromosome 13 at a comparable distance from the *PV31* homologue as the other two *MRP* genes (Table 1).

The three soybean *MRP* genes share a high degree of homology (93% between *Gm03g32500* and *Gm19g35230* and *c.* 86% between *Gm13g18960* and *Gm19g35230*) and are located in syntenic regions (Fig. S1).

Identification of *PvMrp1* and *PvMrp2*, cosegregation analysis and mapping

To verify if the *lpa1*(280-10) mutant was linked to a defective orthologue of one of the soybean MRP genes described
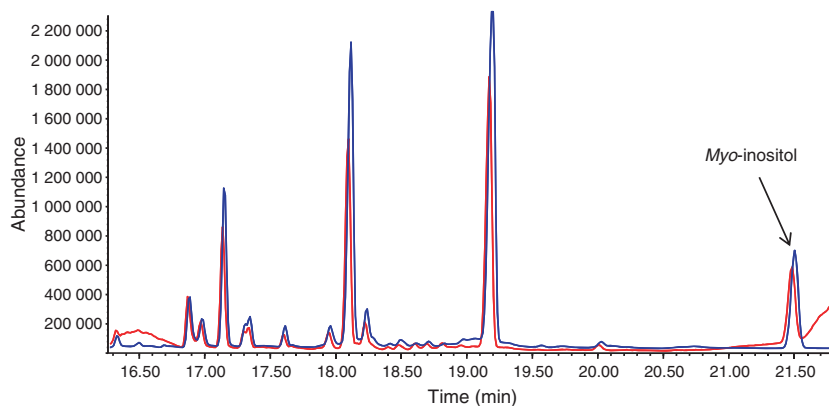
Fig. 2 Gas chromatography/mass spectrometry (GC/MS) analysis of myo-inositol content in wild-type (wt) and lpa1(280-10) seeds. The myo-inositol traces of wt and lpa1(280-10) extracts are indicated by the blue and red lines, respectively. The peak corresponding to myo-inositol is indicated by the arrow. Myo-inositol was quantified as a hexa-trimethylsilyl ether derivative and was identified by comparing the mass fragmentation pattern with the database library NIST05 and quantified by standard curve (obtained using the external standard method).
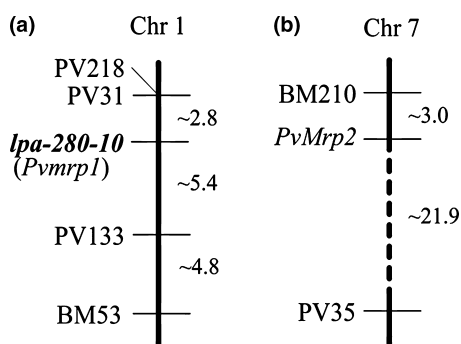

Fig. 3 Mapping of PvMrp1 and PvMrp2 genes. (a) Mapping of lpa1(280-10) (Pvmrp1) mutation. Approximate distance of lpa1(280-10) from PV31, PV218, PV133 and BM53 simple sequence repeat molecular markers is shown on chromosome 1 (Chr 1). (b) Mapping of PvMrp2 sequence. The approximate distance of PvMrp2 from BM210 and PV35 SSR molecular markers is shown on chromosome 7 (Chr 7). Genetic distances are expressed in cM.

earlier, we needed to isolate common bean MRP orthologous sequences from which to design allele-specific primers. To this purpose, we screened a BAC library (Galasso et al., 2009) and found four positive clones, containing two types of MRP sequences: one named PvMrp1, with greatest similarity to Gm03g32500 and Gm19g35230, and another named PvMrp2, with higher homology to Gm13g18960.

Cosegregation analysis was performed using allele-specific primers designed for both PvMrp1 and PvMrp2 to verify if one of the two genes is associated with the lpa phenotype. For PvMrp1, gene-specific amplifications of 140 bp for the Mrp1(280-10) allele and 125 bp for the wt allele Mrp1(Jalo EEP558) were obtained using pol_19.03f and pol_19.04r primers. For the PvMrp2 gene, gene-specific amplifications of 131 bp for the Mrp2(280-10) allele and 122 bp for the Mrp2(Jalo EEP558) allele were obtained using pol1F and pol1R primers. The genotyping, performed on 173 lpa

mutants, from the described F_2 mapping population, showed that all the samples analysed were homozygous for the Mrp1(280-10) allele, thus indicating the PvMrp1 gene as a likely candidate for the lpa mutation (Fig. 3a). Conversely, in the same mutant individuals, the PvMrp2 alleles showed independent assortment.

To further confirm this finding, the same strategy used for mapping the lpa1 mutation was used for the PvMrp2 sequence. Both bulks were amplified using the 19 polymorphic SSRs (Table S1). Since the BM210 and PV35 markers showed a clear bias toward a sequence-specific band in bulk B (homozygous for the 131 bp band) as compared with bulk A (homozygous for the 122 bp band), the PvMrp2 sequence could be located on chromosome 7. PvMrp2 was then mapped by analysis of the distribution of BM210 and PV35 markers in 145 individuals from the F_2 segregating population, and its position was estimated at a distance of 3 cM from BM210 and 21.9 cM from PV35 (Fig. 3b).

PvMrp1 (Lpa1) and PvMrp2 genes codes for highly orthologous proteins

Based on sequence data of soybean Gm03g32500, Gm19g35230 and Gm13g18960 MRP genes, the bean PvMrp1 and PvMrp2 genes and their complementary DNA (cDNA) were isolated from both lpa1(280-10) and wt plants. Genomic and cDNA sequencing showed that PvMrp1 is composed of 11 exons and 10 introns, and according to the deduced open reading frame, encodes a protein of 1538 amino acids (Fig. 4a). Sequencing of PvMrp2 is not complete yet, but, according to results obtained thus far, it shares the same intron-exon structure with PvMrp1 (Fig. 4a). Both genes have the same intron-exon structure of their soybean homologues and the main difference is the length of corresponding introns (Fig. 4a,

Table 1 Mapping of simple sequence repeat markers *PV31* and *PV133* on soybean chromosomes

PV133	e-value	PV31	Distance between *PV133* and *PV31* (bp)	Position of Gm *MRP* gene	e-value	Distance from of Gm *MRP* gene from *PV31* (bp)
Gm03: 37869831..37870034	2.60E-72	Gm03: 41203550..41203746	3333516	Gm03:40213095..40220883	1.50E-51	982667
Gm19: 40445808..40446022	9.80E-59	Gm19:43719523..43719669	3273501	Gm19:42756966..42764732	1.20E-46	954791
Gm07: 13980910..13981076	4.20E-38	Gm13:23669557..23669724	–	Gm13:22555922..22564350	1.00E-15	1105207
Gm14: 30465240..30465132	3.70E-26	Gm10:4605169..4605296	–	nd	1.60E-13	–
Gm06: 36944898..36945013	1.30E-25	nd	–	nd	–	–

Blast positions and corresponding e-value are given for each positive match. The position of soybean *MRP* genes found close to one or both markers is also shown.
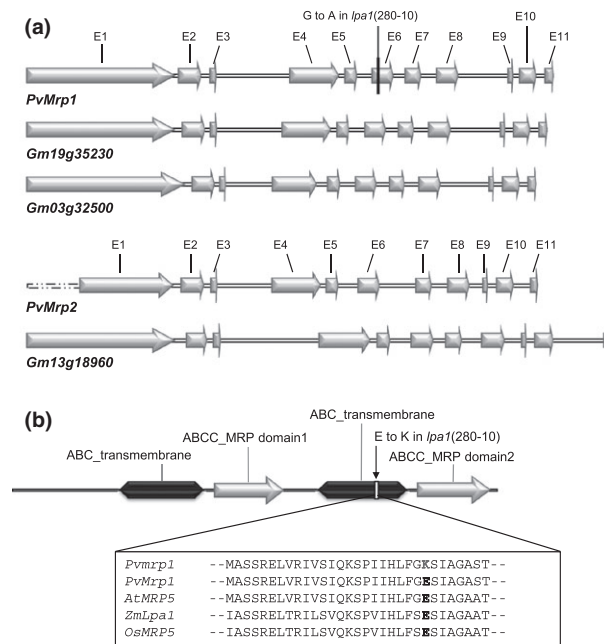

Fig. 4 (a) Schematic diagram showing the exon-intron structure of *PvMrp1* and *PvMrp2* genes and their corresponding soybean homologues, *Gm03g32500*, *Gm19g35230* and *Gm13g18960*. Arrows represent exons (E1–E11); connecting lines represent introns. The vertical bar indicates the Glu$_{1155}$ to Lys$_{1155}$ amino acid change that occurred in exon 6 of *Pvmrp1* gene. The dotted line represents the missing part of exon 1 in *PvMrp2* gene. (b) Predicted structure of the PvMRP1 protein, which is 1538 amino acids long. The two copies of each ABC_transmembrane and ABCC_MRP domain are represented by black boxes and white arrows. The position of the *lpa1*(280-10) mutation is shown. The multiple alignment of the corresponding amino acid region where the amino acid change occurred in orthologous multidrug resistance proteins from *Arabidopsis*, maize and rice, is shown in the linked box.

compare *PvMrp1* with *Gm03g32500* and *Gm19g35230* and *PvMrp2* with *Gm13g18960*).

In silico conserved domain analysis (Marchler-Bauer *et al.*, 2009) confirmed the presence of typical MRP modular structures, comprising two transmembrane domains (ABC_transmembrane), each followed by a nucleotide-binding domain (ABCC_MRP domain) (Fig. 4b) (Rea, 2007).

Sequence comparison between the candidate *Mrp1*(280-10) and wt *Mrp1*(905) alleles showed a single base pair change (G/C-A/T transition) in the sixth exon (Fig. 4a), causing an amino acid change from Glu to Lys at position 1155. In order to confirm this point mutation, the surrounding sequence (amplicon 19.R, Table S2) was amplified and sequenced from 50 different bean genotypes of our collection; no polymorphisms were found (data not shown). Moreover, a BLASTp search and subsequent multiple alignment using the translated *PvMrp1* protein against the green plants database, showed that the Glu$_{1155}$ residue is highly conserved, present in 99 out of the 100 most similar hits (in the other it was replaced by Asp).

Interrogation of the Conserved Domain Database tool at the National Center for Biotechnology Information (NCBI) located the mutation in the second ABC_transmembrane domain. Moreover, alignment of the peptide sequence of *PvMrp1* with the three-dimensional structure of the model ABC transporter mouse P-glycoprotein (PDP ID: 3G5U_A) suggests that Glu_{1155} locates on the inside face of the transmembrane domain, towards the cytosolic side, close to the second ATP binding domain (Fig. S2).

The discovery of the highly similar paralogue *PvMrp2* gene raised the question whether it was expressed in developing seeds. Semiquantitative RT-PCR of *PvMrp1* and *PvMrp2* expression in wt and *lpa1*(280-10) developing seeds as well as in leaves and roots showed that both genes are expressed during seed development, roots, leaves (Fig. 5) and other green tissues (data not shown), suggesting that both PvMRP1 and PvMRP2 proteins are synthesized in all the tissues and developmental conditions analysed. Interestingly, *Pvmrp1* and *PvMrp2* expression appears to be differently regulated in leaves and roots of *lpa1* plants, compared with the wt, indicating that further investigation is needed to address this point.

The *lpa1* mutation causes a negative feedback regulation on the phytic acid pathway

Analysis of phytate content in developing seeds revealed that $InsP_6$ was not detected at any time during seed development in *lpa1*(280-10), while, by contrast, phytate accumulation was already evident in the wt at 18 DAF (Fig. 1a,b). Suppressed ion conductivity is a much less sensitive technique than radiolabelling, and thus, while we did not detect accumulation of phytate, even in storage tissue, the *lpa1*(280-10) mutant still retains the ability to synthesize $InsP_6$, as shown by *in vivo* labelling of mature leaves and developing seeds with *myo*-[2-^{3}H]inositol (Fig. 6). The low concentrations of radiolabelled InsPs achieved precluded

Fig. 6 High-performance liquid chromatography (HPLC) profiles of extracts from *myo*-[2-^{3}H]inositol-labelled leaves (a) and developing seeds (b, c). Inositol phosphates in mature leaves labelled for 72 h (wt, black line; *lpa1*(280-10), grey line) (a). Conductivity profiles (grey lines) and radioactivity traces (black lines) of inositol phosphates from developing seeds at 18 d after flowering (DAF): wt (b), *lpa1*(280-10) (c). Arrows indicate peaks of phytic acid ($InsP_6$) (a–c); the arrowhead indicates $InsP_2$, stereoisomer(s) unidentified (a). In (a), data collection for wt commenced 1 min after injection of the sample. In (b) and (c), the conductivity trace is offset by +0.5 min to accommodate the plumbing delay between the conductivity and the radioactivity detectors.
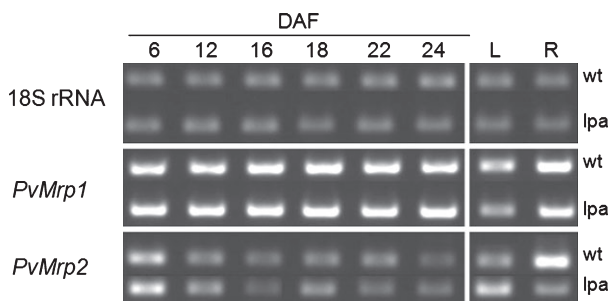

Fig. 5 Expression analysis of *PvMrp1* and *PvMrp2* genes in wild-type (wt) and *lpa1*(280-10) plants. Semiquantitative reverse transcription polymerase chain reaction (RT-PCR) analysis was performed on total RNA isolated from developing seeds (6–24 d after flowering (DAF)), leaves (L) and roots (R). The 18S rRNA was used as control.
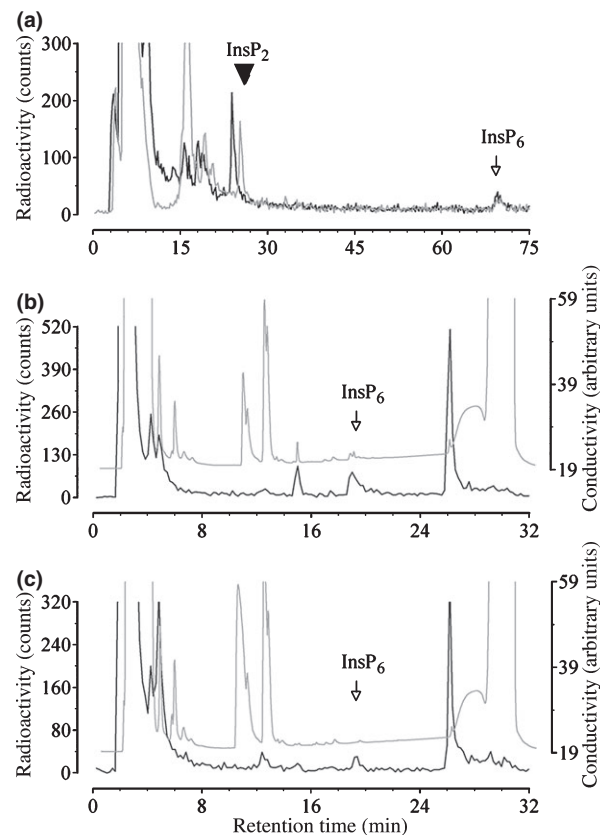
their stereoisomeric analysis. We think it possible that the major peak of labelling evident at the retention time of 26 min for developing beans of both wt and *lpa1*(280-10) is an $InsP_2$.

The lack of substantial accumulation of phytate in seeds of *lpa1*(280-10) indicates the existence of regulatory mechanisms to control the accumulation of cytosolic phytate that might involve negative feedback, whereby $InsP_6$ might function as a feedback signal to repress its own biosynthetic pathway, as has been suggested by Shi *et al.* (2007).

To confirm or deny this hypothesis we performed a transcriptional analysis of a set of structural genes, shown to be involved in $InsP_6$ synthesis in various plants, during wt and *lpa1*(280-10) seed development (Fileppi *et al.*, 2010). We also undertook a protein blot analysis for MIPS using antibodies developed against recombinant PvMIPSs protein
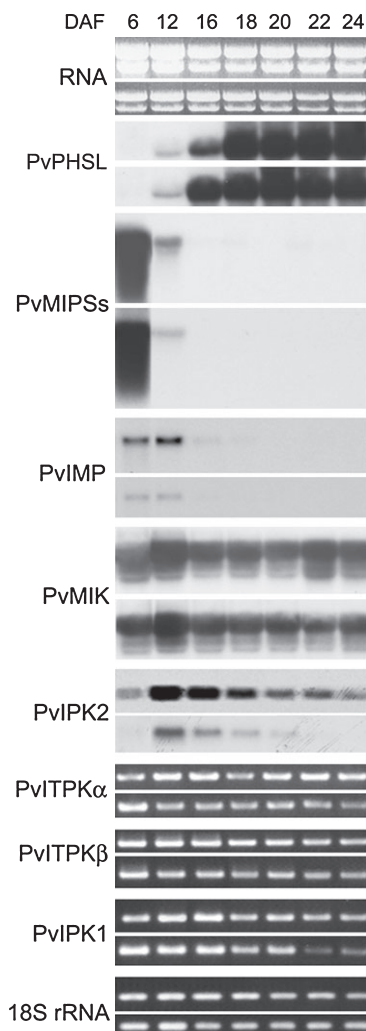
Fig. 7 Expression analysis of genes of the phytic acid pathway during wild-type (wt) and *lpa1*(280-10) seed development. For Northernblot analyses, total RNAs (10 μg for each sample) from wt and *lpa1*(280-10) developing seeds (from 6 to 24 d after flowering (DAF)) were loaded on to the same gel and blotted on the same membrane. This membrane was then hybridized with the different probes as follows: *PvMIPSs*, *PvIMP*, *PvMIK*, *PvIPK2* and *PvPHSL*. The latter one, coding for phaseolin storage protein, was used as an additional control. In fact, we assumed that phaseolin expression would not be affected by the *lpa1*(280-10) mutation. Semiquantitative reverse transcription polymerase chain reaction (RT-PCR) was performed on *PvITPKα*, *PvITPKβ*, *PvIPK1* and 18S rRNA. For each gene the upper panel refers to the wt, while the lower one refers to the *lpa1*(280-10) mutant.

(Fig. S3, Methods S1). In addition, each considered gene was sequenced as both cDNA and genomic DNA in order to exclude the occurrence of ethane methyl sulfonate (EMS)-induced point mutations in the *lpa1*(280-10) mutant.

None of the analysed genes showed sequence differences between wt and *lpa1*(280-10) line (data not shown). However, at the transcriptional level there was a broad effect of the mutation on key genes for the synthesis of InsP$_6$. Some

genes (*PvMIPSs*, *PvIMP*, *PvIPK2* and *PvIPK1*) were down-regulated in the mutant compared with the wt, although to different extents. In fact, while *PvMIPSs* and *PvIPK1* expression was slightly reduced in the mutant, *PvIMP* and *PvIPK2* were more repressed (Fig. 7). In the absence of detailed analysis of metabolite pool sizes and of the pathway flux in mutant and wt, it is particularly difficult to predict the influence of the *lpa1*(280-10) mutation on individual reactions catalysed by enzymes encoded by genes with reduced transcripts. For instance, protein blot analysis of PvMIPS expression showed that, although the encoding gene is slightly down-regulated in the *lpa1*(280-10) mutant, this does not hold true for the protein, which was detectable at the same level in both mutant and wt developing seeds (Fig. 3Sb). Our interpretation is further hampered by limited evidence of the physiological substrate(s) of these enzymes, particularly in the case of inositol phosphate kinases.

Enhanced sensitivity of *lpa1*(280-10) seeds toward ABA-mediated germination

To verify if the low amount of *myo*-inositol found in the *lpa1*(280-10) seeds was correlated to their response to ABA during seed germination, we carried out germination tests. Our results indicate that after 3 d of germination, the *lpa1*(280-10) mutant displayed 35% inhibition of germination at 50 μM of ABA, compared with a figure of 84% for the wt, thus indicating an increased sensitivity to ABA of the mutant (Fig. 8).

Discussion

Several *lpa* mutants have been isolated in many crops and for a number of them the mutated gene has been identified.
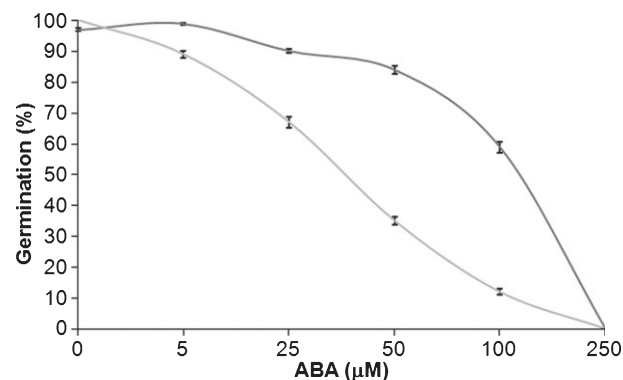

Fig. 8 Abscisic acid (ABA) dose–response curve for germination inhibition of wild-type (wt, black line) and *lpa1*(280-10) (grey line) seeds. Reported percentages of germination were recorded after 3 d of germination in the presence of different ABA concentrations (2.5, 5, 25, 50, 100, 250 μM). Bars indicate standard errors of the means from three independent experiments, each consisting of 100 seeds.

Among the stronger *lpa* mutants are those carrying a defective $InsP_6$ transporter; however, the effects of each mutation on plant physiology may be quite different.

Here, we provide evidence that the bean *lpa1*(280-10) mutant, which is viable and agronomically robust, carries a defective *PvMrp1* gene. This mutation was previously reported to result in an almost complete block of $InsP_6$ accumulation and a 25% reduction in seed raffinosaccharide content (Campion *et al.*, 2009). Furthermore, we detected a 30% reduction of *myo*-inositol content that may underlie the ABA hypersensitive response found during *lpa1*(280-10) seed germination. These data, together with the results of the expression analyses of genes involved in $InsP_6$ biosynthesis, demonstrate that the *mrp1* mutation accompanies a general repression of its pathway. We propose that failure to accumulate phytate in storage organelles has consequences for cytosolic $InsP_6$ that, directly or indirectly, reduces its biosynthesis through a negative feedback mechanism which manifests in altered *myo*-inositol content of mature seeds.

Common bean and soybean contain two *MRP* genes orthologous to known $InsP_6$ transporters

Because of the high degree of synteny existing between soybean and common bean, we could map and identify the mutated gene. Furthermore, we demonstrated the existence of a second highly conserved MRP orthologous gene (*Gm13g18960* and *PvMrp2*) in these two crops. The proteins coded by these two orthologues share > 80% similarity with PvMRP1 orthologues, a much higher similarity than that shared with AtMRP5 and ZmMRP4 proteins (Fig. S4). This finding strongly suggests that the MRP2 protein might be a $InsP_6$ transporter too. However, despite the coexpression of *PvMrp1* and *PvMrp2* in developing seeds, mutation of *PvMrp1* is sufficient to confer a *lpa* phenotype on the *lpa1*(280-10) mutant. Although *PvMrp2* does not complement the *lpa1*(280-10) mutation in seeds, even if it shares to some extent the expression pattern with *PvMrp1*, a hypothetical functional similarity cannot be excluded. A different post-transcriptional regulation or intracellular localization could still explain the lack of functional complementation between the two MRP paralogues in seeds. As for other tissues, a detectable phenotype of the mutated *Pvmrp1* could not be found. In this regard, the lack of negative pleiotropic effects that *lpa* mutants often displayed in other species could be explained by a *PvMrp2* functional complementation. In fact, according to the phylogenetic analysis of the *MRPs* homologues (Fig. S4), the paralogous duplication that generated *PvMrp1* and *PvMrp2* occurred in a common ancestor of both common bean and soybean, and not in other species, such as the cereals, which display impairing pleiotropic effects when their single MRP homolog is mutated. Similar

conclusions can be drawn for the soybean mutant CX1834, in which it has been shown that mutations in *Gma03g32500* and *Gma19g35230* genes, orthologous of *PvMrp1*, are sufficient to confer a *lpa* phenotype. However, we cannot further compare the two species, since no expression data of *Gma13g18960*, the *PvMrp2* orthologue, are available in soybean. Moreover, while we have no data on PvMRP2 protein synthesis in developing seeds, further characterization of this second gene may yet reveal novel functions for $InsP_6$ transporters and thus this gene deserves much attention.

Sequencing data showed that the *PvMrp1* gene underwent a nucleotide substitution that predicts an amino acid change from Glu_{1155} to Lys_{1155} in a highly conserved position in plant MRPs proteins. Based on the alignment with the structure of the mouse P-glycoprotein, a multiple drug resistance (MDR) transporter of the ABC superfamily (Aller *et al.*, 2009), this amino acid substitution is presumably located in the inner face of the second transmembrane domain toward the cytosolic side. Considering that the effect of this mutation is an almost complete disappearance of phytate in *lpa1*(280-10) bean seeds, we may speculate that the dramatic substitution, from an acidic to a basic residue, has occurred in a position that might be involved in ligand interaction, relevant for the recognition and/or transport of $InsP_6$. Detailed studies on the structure of PvMRP1 (or orthologous proteins from other species) are needed to address the role of Glu_{1155} in the transport of $InsP_6$.

Effects of *PvMrp1* mutation on inositol phosphate metabolism and the role of *myo*-inositol

The evidence collected demonstrates that in *lpa1*(280-10) seeds and leaves, $InsP_6$ is still synthesized. In the absence of transport we would expect $InsP_6$ to accumulate in the cytosolic compartment. We were, however, unable to detect $InsP_6$ at any stage of seed development by suppressed ion conductivity (Figs 1, 6). It is worth noting that, while others (Bentsink *et al.*, 2003) have reported measurement of $InsP_6$ in nonstorage tissues (e.g. leaves by suppressed ion conductivity), our own analysis of leaf tissue of *Atmrp5* and bean *lpa1*(280-10) did not allow us to distinguish phytate from interferences.

Considering cytosolic phytate, Veiga *et al.* (2006) made a theoretical estimate of phytate solubility and set the limiting value at a concentration of 49 μM, above which any $InsP_6$ precipitates as magnesium phytate. This concentration is well below the one present in the globoids of mature seeds, the vacuolar subcompartment in which $InsP_6$ is normally stored. Assuming that the plant cell cannot accumulate and/or manage large amounts of phytate salts in the cytosol, it is likely that cytosolic phytate concentrations are regulated, in part, by degradative processes, mediated by the action of phosphatases and phytases, which, together with

the synthetic process, modulates turnover. This is evident in the stereoisomeric profile of InsPs identified, for example, in aleurone tissue of imbibing de-embryonated barley grains (Brearley & Hanke, 1996) in which the radiolabelled intermediates were identical to the products of *in vitro* phytate degradation by bran phytases (reviewed in Irving, 1980). It is therefore possible to speculate that any regulation of turnover of cytosolic phytate, by $InsP_6$ dephosphorylation and/or negative feedback on $InsP_6$ synthesis, is already operative in the micromolar range.

Coelho *et al.* (2005) showed that $InsP_6$ synthesis in developing bean seeds is maximal at 22 d after pollination, suggesting that $InsP_6$ synthesis begins early in seed development. Newly synthesized $InsP_6$ is expected to increase with the progression of seed development and if it cannot be stored in the cytosol as phytate salts, it may be degraded to *myo*-inositol and free phosphate. We speculate that this could cause a transient increase in *myo*-inositol that will negatively regulate the expression of genes and or enzymes controlling $InsP_6$ biosynthesis as well as the *myo*-inositol cellular pool, as reported to occur in *Catharanthus roseus* (Mitsuhashi *et al.*, 2005). A 31–34% reduction in magnesium content in *Arabidopsis Atmrp5* mutants has been reported by Nagy *et al.* (2009). Since Mg^{2+} is known to be an essential activator of *myo*-inositol-phosphate monophosphatase (IMP) (Atack *et al.*, 1995; Islas-Flores & Villanueva, 2007), it is possible that a decrease of the intracellular concentration of Mg^{2+} may further affect IMP activity/expression.

One interpretation of our data is that $InsP_6$, or a product of its turnover, regulates the transcription of genes coding for key enzymes of phytic acid pathway, as already suggested by Shi *et al.* (2007). In maize *lpa1-1* and its allelic mutant *lpa1-241*, a consistent reduction of *MIPS* gene expression was reported (Raboy *et al.*, 2000; Pilu *et al.*, 2003). We observed a slight reduction of *PvMIPS* transcript and no changes in MIPS protein expression (Fig. 3S). Conversely, we found a strong inhibition of *PvIMP* transcription that would be expected to strongly reduce *myo*-inositol content. The fact that the *myo*-inositol content of mature *lpa1*(280-10) seeds is only 30% lower than in the wt, may be explained if *myo*-inositol concentrations are raised by a futile cycle in which $InsP_6$ is continuously synthesized from and dephosphorylated to *myo*-inositol (Fig. 9). In this context, the presence of lower InsPs which retain the 2-phosphate are diagnostic markers of $InsP_6$ turnover (Brearley & Hanke, 1996). The limited extent of labelling of lower InsPs that we observed, however, precluded stereoisomeric analysis.

Reduction of phytate accumulation in many *lpa* mutants is often correlated with pleiotropic effects which frequently affect seed germination and field emergence, seed filling, biotic and abiotic stress responses and protection from oxidative stress (Keller *et al.*, 1998; Klein *et al.*, 2003; Meis *et al.*, 2003; Pilu *et al.*, 2005; Bregitzer & Raboy, 2006; Guttieri *et al.*, 2006; Murphy *et al.*, 2008; Doria *et al.*, 2009; Meng *et al.*, 2009). Changes in root development and root hair growth, phosphate sensing, ABA and IAA

Fig. 9 Proposed model for *myo*-inositol recycling in the *lpa1*(280-10) mutant and effect of the *lpa1*(280-10) mutation on phytic acid and raffinosaccharides pathways. The *lpa1*(280-10) mutant has a $Ins(1,2,3,4,5,6)P_6$ defective transporter (indicated with a black cross). However, $InsP_6$ is still synthesized, but, since it cannot be stored correctly in the vacuole, it is degraded by phytases back to *myo*-inositol, giving rise to a futile cycle (grey dotted line). This causes a negative feedback regulation of key genes of phytic acid pathway and a consequent decrease of *myo*-inositol and raffinosaccharides (grey boxes). Light and dark grey boxes indicate lower and higher transcriptional repression, respectively. PtdIS, phosphatydil inositol phosphate synthase; PtdI4K, phosphatydil inositol 4-kinase; PtdI5K, phosphatydil inositol 5-kinase; PtdIns, phosphatydil inositol; PtdIns(4)P_1, phosphatydil inositol 4-phosphate; PtdIns(4,5)P_2, phosphatydil inositol 4,5-biphosphate.
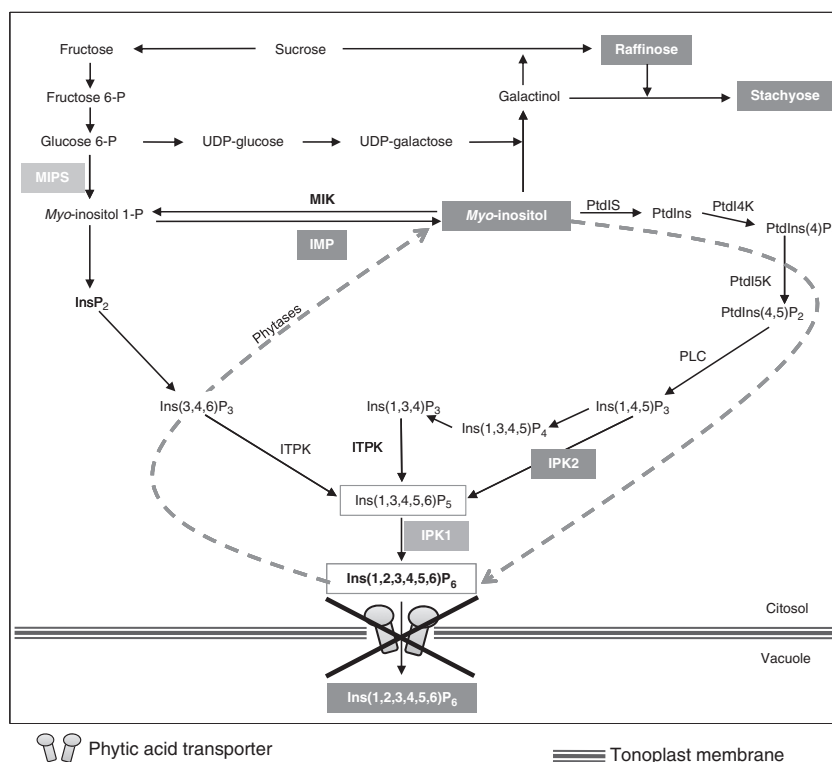
response have also been reported (Gaedeke *et al.*, 2001; Klein *et al.*, 2003; Stevenson-Paulik *et al.*, 2005). Nagy *et al.* (2009) showed that, as for wt, phytate synthesis in *Atmrp5* seedlings, recorded as incorporation of *myo*-[^{3}H]-inositol, was reduced under P$_i$-limiting conditions; while Murphy *et al.* (2008) showed the converse, that phytate accumulation in potato tubers was enhanced by supplementation of *myo*-inositol. Mitsuhashi *et al.* (2005) showed that vacuolar phytate accumulation is enhanced in suspension cultures of both *Catharanthus roseus* and *Arabidopsis* in conditions of elevated external phosphate supply. All these pleiotropic effects reveal complex integration of inositol, phytate and phosphate status. They are not unexpected considering that *myo*-inositol, its phosphorylated derivatives and InsP$_6$ itself play a central role in several metabolic processes and in signal transduction (Loewus & Murthy, 2000). Indeed, *myo*-inositol biosynthesis and conversion must be a highly controlled and regulated process in order to meet the requirements of the different pathways in which this compound is involved.

The expression and protein blot data for *PvMIPS* do not suggest major differences in *myo*-inositol-3-phosphate content of mature wt and *lpa1*(280-10), while the strong repression observed for *PvIMP* gene seems to be in agreement with the reduction in *myo*-inositol detected in mature *lpa1*(280-10) seeds (Fig. 2). This reduction is similar to that observed in maize *lpa1-241* (Pilu *et al.*, 2003). Interestingly, the maize *lpa1-1* mutant, allelic to *lpa1-241*, accumulates more *myo*-inositol than wt seeds (Shi *et al.*, 2007). A similar behaviour was found for the two allelic *mrp5* mutants of rice, *Os-lpa-XS110-2* and *Os-lpa-XS110-3*, which have lower and higher *myo*-inositol than wt, respectively (Xu *et al.*, 2009). Alterations in *myo*-inositol content have also been reported in other *lpa* mutants: *mik* mutants, such as maize *lpa3* and rice *Os-lpa-XS110-1* and *lpa N15-186*, contain higher seed *myo*-inositol (Shi *et al.*, 2005; Kim *et al.*, 2008; Xu *et al.*, 2009); conversely decreased *myo*-inositol is typically found in *mips* transgenics, *mips* and *vtc4* mutants (Keller *et al.*, 1998; Hitz *et al.*, 2002; Torabinejad *et al.*, 2009; Donahue *et al.*, 2010). These findings indicate complex regulation of seed *myo*-inositol content, which, presumably, reflects the integration of a number of metabolic pathways which draw on *myo*-inositol and *myo*-inositol-3-phosphate. We conclude that the different content of seed *myo*-inositol does not seem to correlate exclusively with the strength of the *lpa* phenotype, suggesting that the regulation of *myo*-inositol content might be more complicated than expected and should involve several as yet unknown factors.

What is clear from our results and recently published papers on *Arabidopsis mips1* and *vtc4* mutants and *AtPAP15* overexpressing lines, is that the concentration of *myo*-inositol found in mature seeds correlates with the response to ABA during seed germination (Zhang *et al.*, 2008;

Torabinejad *et al.*, 2009; Donahue *et al.*, 2010). In these mutants, *myo*-inositol changes are directly correlated with changes in ascorbic acid content and the displayed altered response to ABA is purported to depend on the capacity of the mutants to cope with reactive oxygen species (ROS). In agreement with this hypothesis is the finding that the maize *lpa1-241*, which has a 40% decrease in seed *myo*-inositol, also shows increased sensitivity to oxidative stress (Doria *et al.*, 2009). We do not have specific data on the response of bean *lpa1*(280-10) to oxidative stress; however, we showed that this mutant is viable, shows no negative pleiotropic effects affecting traits of agronomic relevance and does not differ from wt plants in the response to drought stress (D. Panzeri *et al.*, unpublished). Experiments are in progress aiming to assay *myo*-inositol, *myo*-inositol monophosphate and ascorbic acid content both in leaves and during the entire course of seed maturation.

In conclusion, our results provide evidence that contrasting pleiotropic effects of *lpa* mutants carrying a defective InsP$_6$ transporter are linked to the *myo*-inositol content.

Acknowledgements

References

Aller SG, Yu J, Ward A, Weng Y, Chittaboina S, Zhuo R, Harrell PM, Trinh YT, Zhang Q, Urbatsch IL et al. 2009. Structure of P-glycoprotein reveals a molecular basis for poly-specific drug binding. *Science* **323**: 1718–1722.

Atack JR, Broughton HB, Pollack SJ. 1995. Structure and mechanism of inositol monophosphatase. *FEBS Letters* **361**: 1–7.

Bentsink L, Yuan K, Koornneef M, Vreugdenhil D. 2003. The genetics of phytate and phosphate accumulation in seeds and leaves of *Arabidopsis thaliana*, using natural variation. *Theoretical and Applied Genetics* **106**: 1234–1243.

Bohn L, Josefsen L, Meyer AS, Rasmussen SK. 2007. Quantitative analysis of phytate globoids isolated from wheat bran and characterization of their sequential dephosphorylation by wheat phytase. *Journal of Agriculture and Food Chemistry* **55**: 7547–7552.

Brearley CA, Hanke DE. 1996. Metabolic evidence for the order of addition of individual phosphate esters in the *myo*-inositol moiety of inositol hexakisphosphate in the duckweed *Spirodela polyrhiza* L. *The Biochemical Journal* **15**: 227–233.

Bregitzer P, Raboy V. 2006. Effects of four independent low-phytate mutations on barley agronomic performance. *Crop Science* **46**: 1318–1322.

Campion B, Sparvoli F, Doria E, Tagliabue G, Galasso I, Fileppi M, Bollini R, Nielsen E. 2009. Isolation and characterisation of an *lpa* (low

phytic acid) mutant in common bean (*Phaseolus vulgaris* L.). *Theoretical and Applied Genetics* 118: 1211–1221.

Casaravilla C, Brearley C, Soule S, Fontana C, Veiga N, Bessio MI, Ferreira F, Kremer C, Diaz A. 2006. Characterization of *myo*-inositol hexakisphosphate deposits from larval *Echinococcus granulosus*. *FEBS Journal* 273: 3192–3203.

Choi HK, Mun JH, Kim DJ, Zhu HY, Baek JM, Mudge J, Roe B, Ellis N, Doyle J, Kiss GB *et al.* 2004. Estimating genome conservation between crop and model legume species. *Proceedings of the National Academy of Sciences, USA* 101: 15289–15294.

Cichy KA, Raboy V. 2009. Evaluation and development of low phytate crops. In: Krishnan H, ed. *Modification of seed composition to promote health and nutrition*. Madison, WI, USA: American Society of Agronomy and Crop Science Society of America, 177–201.

Coelho CMM, Tsai SM, Vitorello VA. 2005. Dynamics of inositol phosphate pools (tris-, tetrakis- and pentakisphosphate) in relation to the rate of phytate synthesis during seed development in common bean (*Phaseolus vulgaris*). *Journal of Plant Physiology* 162: 1–9.

Donahue JL, Alford SR, Torabinejad J, Kerwin RE, Nourbakhsh A, Ray WK, Hernick M, Huang XY, Lyons BM, Hein PP *et al.* 2010. The *Arabidopsis thaliana Myo-Inositol 1-Phosphate Synthase1* gene is required for *myo*-inositol synthesis and suppression of cell death. *Plant Cell* 22: 888–903.

Doria E, Galleschi L, Calucci L, Pinzino C, Pilu R, Cassani E, Nielsen E. 2009. Phytic acid prevents oxidative stress in seeds: evidence from a maize (*Zea mays* L.) *low phytic acid* mutant. *Journal of Experimental Botany* 60: 967–978.

Dorsch JA, Cook A, Young KA, Anderson JM, Bauman AT, Volkmann CJ, Murthy PP, Raboy V. 2003. Seed phosphorus and inositol phosphate phenotype of barley low phytic acid genotypes. *Phytochemistry* 62: 691–706.

Fileppi M, Galasso I, Tagliabue G, Daminati MG, Campion B, Doria E, Sparvoli F. 2010. Characterisation of structural genes involved in phytic acid biosynthesis in common bean (*Phaseolus vulgaris* L.). *Molecular Breeding* 25: 453–470.

Gaedeke N, Klein M, Kolukisaoglu U, Forestier C, Müller A, Ansorge M, Becker D, Mamnun Y, Kuchler K, Schulz B *et al.* 2001. The *Arabidopsis thaliana* ABC transporter AtMRP5 controls root development and stomata movement. *EMBO Journal* 20: 1875–1887.

Galasso I, Piergiovanni AR, Lioi L, Campion B, Bollini R, Sparvoli F. 2009. Genome organization of Bowman-Birk inhibitor in common bean (*Phaseolus vulgaris* L.). *Molecular Breeding* 23: 617–624.

Gillman JD, Pantalone VR, Bilyeu K. 2009. The low phytic acid phenotype in soybean line CX1834 is due to mutations in two homologs of the maize low phytic acid gene. *The Plant Genome* 2: 179–190.

Grisi MCM, Blair MW, Gepts P, Brondani C, Pereira PAA, Brondani RPV. 2007. Genetic mapping of a new set of microsatellite markers in a reference common bean (*Phaseolus vulgaris*) population BAT93 × Jalo EEP558. *Genetics and Molecular Research* 6: 691–706.

Guttieri MJ, Peterson KM, Souza EJ. 2006. Agronomic performance of low phytic acid wheat. *Crop Science* 46: 2623–2629.

Hambidge KM, Huffer JW, Raboy V, Grunwald GK, Westcott JL, Sian L, Miller LV, Dorsch JA, Krebs NF. 2004. Zinc absorption from low-phytate hybrids of maize and their wild-type isohybrids. *American Journal of Clinical Nutrition* 79: 1053–1059.

Hambidge KM, Krebs NF, Westcott JL, Sian L, Miller LV, Peterson KL, Raboy V. 2005. Absorption of calcium from tortilla meals prepared from low-phytate maize. *American Journal of Clinical Nutrition* 82: 84–87.

Hatzack F, Hubel F, Zhang W, Hansen PE, Rasmussen SK. 2001. Inositol phosphates from barley low-phytate grain mutants analyzed by metal-dye detection HPLC and NMR. *Biochemical Journal* 354: 473–480.

Hitz WD, Carlson TJ, Kerr PS, Sebastian SA. 2002. Biochemical and molecular characterization of a mutation that confers a decreased

raffinosaccharide and phytic acid phenotype on soybean seeds. *Plant Physiology* 128: 650–660.

Irving GCJ. 1980. Phytase. In: Cosgrove DJ, ed. *Studies in organic chemistry 4. Inositol phosphates: their chemistry, biochemistry, and physiology*. Amsterdam, the Netherlands: Elsevier Science Ltd, 85–98.

Islas-Flores I, Villanueva MA. 2007. Inositol-1 (or 4)-monophosphatase from *Glycine max* embryo axes is a phosphatase with broad substrate specificity that includes phytate dephosphorylation. *Biochimica Et Biophysica Acta-General Subjects* 1770: 543–550.

Keller R, Brearley CA, Trethewey RN, Muller-Rober B. 1998. Reduced inositol content and altered morphology in transgenic potato plants inhibited for 1D-myo-inositol 3-phosphate synthase. *Plant Journal* 16: 403–410.

Kim SI, Andaya CB, Goyal SS, Tai TH. 2008. The rice *OsLpa1* gene encodes a novel protein involved in phytic acid metabolism. *Theoretical and Applied Genetics* 117: 769–779.

Klein M, Perfus-Barbeoch L, Frelet A, Gaedeke N, Reinhardt D, Mueller-Roeber B, Martinoia E, Forestier C. 2003. The plant multidrug resistance ABC transporter AtMRP5 is involved in guard cell hormonal signalling and water use. *Plant Journal* 33: 119–129.

Lander ES, Green P, Abrahamson J, Barlow A, Daly MJ, Lincoln SE, Newburg L. 1987. MAPMAKER: An interactive computer package for constructing primary genetic linkage maps of experimental and natural populations. *Genomics* 1: 174–181.

Loewus FA, Murthy PPN. 2000. myo-inositol metabolism in plants. *Plant Science* 150: 1–19.

Lorence A, Chevone BI, Mendes P, Nessler CL. 2004. *myo*-inositol oxygenase offers a possible entry point into plant ascorbate biosynthesis. *Plant Physiology* 134: 1200–1205.

Marchler-Bauer A, Anderson JB, Chitsaz F, Derbyshire MK, DeWeese-Scott C, Fong JH, Geer LY, Geer RC, Gonzales NR, Gwadz M *et al.* 2009. CDD: specific functional annotation with the Conserved Domain Database. *Nucleic Acids Research* 37 (Suppl. 1): D205–D210.

Meis SJ, Fehr WR, Schnebly SR. 2003. Seed source effect on field emergence of soybean lines with reduced phytate and raffinose saccharides. *Crop Science* 43: 1336–1339.

Mendoza C, Viteri FE, Lonnerdal B, Young KA, Raboy V, Brown KH. 1998. Effect of genetically modified, low-phytic acid maize on absorption of iron from tortillas. *American Journal of Clinical Nutrition* 68: 1123–1127.

Meng PH, Raynaud C, Tcherkez G, Blanchet S, Massoud K, Domenichini S, Henry Y, Soubigou-Taconnat L, Lelarge-Trouverie C, Saindrenan P *et al.* 2009. Crosstalks between *Myo*-inositol metabolism, programmed cell death and basal immunity in *Arabidopsis*. *PLoS ONE* 4: e7364.

Mitsuhashi N, Ohnishi M, Sekiguchi Y, Kwon Y-U, Chang Y-T, Chung S-K, Inoue Y, Reid RJ, Yagisawa H, Mimura T. 2005. Phytic acid synthesis and vacuolar accumulation in suspension-cultured cells of *Catharanthus roseus* induced by high concentration of inorganic phosphate and cations. *Plant Physiology* 138: 1607–1614.

Munnik T, Vermeer JEM. 2010. Osmotic stress-induced phosphoinositide and inositolphosphate signalling in plants. *Plant Cell and Environment* 33: 655–669.

Murphy AM, Otto B, Brearley CA, Carr JP, Hanke DE. 2008. A role for inositol hexakisphosphate in the maintenance of basal resistance to plant pathogens. *Plant Journal* 56: 638–652.

Nagy R, Grob H, Weder B, Green P, Klein M, Frelet-Barrand A, Schjoerring JK, Brearley CA, Martinoia E. 2009. The *Arabidopsis* ATP-binding cassette protein AtMRP5/AtABCC5 is a high affinity inositol hexakisphosphate transporter involved in guard cell signaling and phytate storage. *Journal of Biological Chemistry* 284: 33614–33622.

Pilu R, Landoni M, Cassani E, Doria E, Nielsen E. 2005. The maize *lpa241* mutation causes a remarkable variability of expression and some pleiotropic effects. *Crop Science* 45: 2096–2105.

New
Phytologist

Pilu R, Panzeri D, Gavazzi G, Rasmussen SK, Consonni G, Nielsen E. 2003. Phenotypic, genetic and molecular characterization of a maize *low phytic acid* mutant (*lpa241*). *Theoretical and Applied Genetics* 107: 980–987.

Raboy V. 2002. Progress in breeding low phytate crops. *Journal of Nutrition* 132: 503S–505S.

Raboy V. 2006. Seed phosphorous and the development of low-phytate crops. In: Turner BL, Richardson AE, Mullaney EJ, eds. *Inositol phosphates: linking agriculture and environment.* Oxfordshire, UK: CAB International, 111–132.

Raboy V, Gerbasi PF, Young KA, Stoneberg SD, Pickett SG, Bauman AT, Murthy PPN, Sheridan WF, Ertl DS. 2000. Origin and seed phenotype of maize *low phytic acid 1-1* and *low phytic acid 2-1*. *Plant Physiology* 124: 355–368.

Rea PA. 2007. Plant ATP-Binding cassette transporters. *Annual Review of Plant Biology* 58: 347–375.

Saghai Maroof MA, Glover NM, Biyashev RM, Buss GR, Grabau EA. 2009. Genetic basis of the low-phytate trait in the soybean line CX1834. *Crop Science* 49: 69–76.

Shi J, Wang H, Hazebroek J, Ertl DS, Harp T. 2005. The maize *low-phytic acid 3* encodes a myo-inositol kinase that plays a role in phytic acid biosynthesis in developing seeds. *Plant Journal* 42: 708–719.

Shi J, Wang H, Schellin K, Li B, Faller M, Stoop JM, Meeley RB, Ertl DS, Ranch JP, Glassman K. 2007. Embryo-specific silencing of a transporter reduces phytic acid content of maize and soybean seeds. *Nature Biotechnology* 25: 930–937.

Slightom JL, Drong RF, Klassy RC, Hoffman LM. 1985. Nucleotide sequences from phaseolin cDNA clones: The major storage proteins from *Phaseolus vulgaris* are encoded by two unique gene families. *Nucleic Acids Research* 13: 6483–6498.

Sparvoli F, Martin C, Scienza A, Gavazzi G, Tonelli C. 1994. Cloning and molecular analysis of structural genes involved in flavonoid and stilbene biosynthesis in grape (*Vitis vinifera* L.). *Plant Molecular Biology* 24: 743–755.

Stevenson-Paulik J, Bastidas RJ, Chiou ST, Frye RA, York JD. 2005. Generation of phytate-free seeds in *Arabidopsis* through disruption of inositol polyphosphate kinases. *Proceedings of the National Academy of Sciences, USA* 102: 12612–12617.

Torabinejad J, Donahue JL, Gunesekera BN, Allen-Daniels MJ, Gillaspy GE. 2009. VTC4 is a bifunctional enzyme that affects myoinositol and ascorbate biosynthesis in plants. *Plant Physiology* 150: 951–961.

van Tunen AJ, Koes RE, Spelt CE, van der Krol AR, Stuitje AR, Mol JN. 1988. Cloning of the two chalcone flavanone isomerase genes from *Petunia hybrida*: coordinate, light-regulated and differential expression of flavonoid genes. *EMBO (European Molecular Biology Organization) Journal* 7: 1257–1263.

Veiga N, Torres J, Domínguez S, Mederos A, Irvine RF, Díaz A, Kremer C. 2006. The behaviour of myo-inositol hexakisphosphate in the presence of magnesium(II) and calcium(II): Protein-free soluble $InsP_6$ is limited to 49 mM under cytosolic/nuclear conditions. *Journal of Inorganic Biochemistry* 100: 1800–1810.

Xu XH, Zhao HJ, Liu QL, Frank T, Engel KH, An GH, Shu QY. 2009. Mutations of the multi-drug resistance-associated protein ABC transporter gene 5 result in reduction of phytic acid in rice seeds. *Theoretical and Applied Genetics* 119: 75–83.

Zhang W, Gruszewski HA, Chevone BI, Nessler CL. 2008. An *Arabidopsis* purple acid phosphatase with phytase activity increases foliar ascorbate. *Plant Physiology* 146: 431–440.

Supporting Information

Additional supporting information may be found in the online version of this article.

Fig. S1 Representation of the synteny in genomic regions between PV31 and PV133 microsatellites and surrounding *Glyma03g32500*, *Glyma13g18960* and *Glyma19g35230* MRP genes.

Fig. S2 Molecular structure of the model ABC transporter mouse P-glycoprotein (PDP ID: 3G5U_A) showing the topology of the protein.

Fig. S3 Expression analysis of *PvMIPS* transcript (a) and protein (b) during wt (upper panel) and *lpa1*(280-10) (lower panel) seed development (4–26 DAF).

Fig. S4 Rooted neighbour-joining tree showing the phylogenetic relationships of MRP proteins and known phytic acid transporters.

Table S1 Description of the set of 47 SSR markers used in the genetic mapping

Table S2 List of overlapping amplicons of the *PvMrp1* and *PvMrp2* genomic sequences

Table S3 Name and 5′–3′ sequence of the primers used for sequencing and cosegregation analysis of *PvMrp1* and *PvMrp2*

Methods S1 Production of anti-PvMIPSs antibodies and protein blot analysis.

Please note: Wiley-Blackwell are not responsible for the content or functionality of any supporting information supplied by the authors. Any queries (other than missing material) should be directed to the *New Phytologist* Central Office.